A time domain Galerkin boundary element method for a heat conduction interface problem

R. Vodička
Technical University of Košice, Civil Engineering Faculty, Slovakia

Abstract

A heat conduction problem with a material or other type interface is solved. The numerical method used includes a boundary element technique presented as a Galerkin boundary element method for the space variables together with convolution quadrature in time. The treatment of the interface conditions enabled them to be formulated in a weak sense, with generally curved interfaces and independent meshing of each side of the interfaces. Results of the examples present influences of non-conformingly meshed interfaces, a comparison with a known analytical solution, and the time evolution of the interface solution with different material properties of the substructures adjacent to the interface.

Keywords: boundary element method, interface problem, non-matching meshes, heat conduction, convolution quadrature.

1 Introduction

Many problems of civil engineering are modeled by initial-boundary value problems (IBVP) for partial differential equations. Numerical algorithms used for their solution may also include methods based on boundary integral equations (BIE). If, in addition, the solved problem includes an interface, e.g. due to different materials in the analyzed structure or for algorithmic reasons such as parallelization, finding an efficient solver for determining the interface solution may be rather involved. Moreover, a time-dependence may even more complicate the task.

WIT Transactions on Modelling and Simulation, Vol 49, © 2009 WIT Press
www.witpress.com, ISSN 1743-355X (on-line)
doi:10.2495/BE090171

The time-dependent problems can be successfully treated by BIE methods. A nice survey of BIE applications for time dependent problems is given by Costabel [1]. Such methods are widely and successfully being used also for numerical modeling of problems in heat conduction.

The formulation of BIEs, which leads to Symmetric Galerkin Boundary Element Method (SGBEM), has already become classical, see Bonnet *et al.* [2]. It has advantages of symmetry of used boundary integral operators and also their discretized forms – matrices used in numerical solution. It also provides nice convergence properties in energetic norms of Sobolev spaces. With time dependence, there appears a question how to resolve this aspect of the problem. It is possible to use complete space-time solution, or to treat the time variables separately, either by integral, usually Laplace, transform or by a time-stepping algorithm.

In the present paper, the approach introduced uses the Galerkin method only for space variables. The time dependence, which includes the use of convolution in the operators of the integral equations, is treated separately by calculation of the convolution quadrature as introduced by Lubich and Schneider [3], which is based on a linear multistep method and uses only the Laplace transform of the time-dependent fundamental solution.

The existence of an interface requires a split of the space domain into several parts in the solution and usually includes domain decomposition techniques to be used as described by Hsiao *et al.* [4] or Wohlmuth [5]. In the present approach, these are applied very naturally: A variational formulation, originally discussed by Carini [6], of the IBVP directly provides a BIE system with interface conditions directly included into the integral equations as an innovation of the original formulation. Moreover, these conditions are satisfied in a weak form, which has an advantage in the numerical solution for the both sides of the interfaces could be discretized separately. A similar algorithm has been presented for the use with elastic interface problems by Hsiao *et al.* [4], Langer *et al.* [7] or Vodička *et al.* [8].

Independent meshing of both sides of an interface requires a special procedure for cross-transferring of the solution, mainly when the interface is curved. The present approach uses the implementation of data transfer with an auxiliary interface mesh referred to as common-refinement mesh; nevertheless there exist also other possibilities which have been discussed, for example, in de Boer *et al.* [9].

The paper is divided into four main parts. In the first one, Section 2, the solved problem of heat transfer is briefly described. Then, in Section 3, the variational solution leading to a system of BIEs is presented and numerically solved in Section 4 by convolution quadrature in time and by a Galerkin method in space. Finally, Section 5 presents two examples with their solution by suggested approach. One of the examples includes a problem with known analytical solution, so that a comparison can be shown. The other example, although without an analytical solution, even defines different materials for sub-domains and jumps in initial conditions along the interfaces.

2 A heat transfer problem with an interface

Let us consider a body defined by a domain $\Omega \subset R^d$ in a fixed Cartesian coordinate system x_i, $i=1,...,d$, with a bounded Lipschitz boundary $\Gamma=\partial\Omega$. Let $\Gamma_S \subset \Gamma$ denote the smooth part of Γ, i.e. excluding corners, edges, points of curvature jumps, etc. Let n denote the outward unit normal vector defined on Γ_S.

The presence of interfaces causes the domain Ω to be split into several parts. For the sake of simplicity, let us divide Ω into two non-overlapping parts Ω^A and Ω^B whose respective boundaries we denote Γ^A and Γ^B. There also exists a common part of both boundaries, let us denote this coupling boundary by Γ_c.

Let us denote the temperature solution of an initial-boundary value heat conduction problem with an interface in each sub-domain Ω^η as $u^\eta(x;t)$ (the superscript η distinguishes the sub-domains, here it can be either A or B), obtained during a time interval $t \in \langle 0;\bar{t} \rangle$. If neither volume heat sources nor convective boundary conditions are considered and each Ω^η is homogeneous, the problem can be formulated as follows:

$$\begin{gathered}
\frac{\partial u^\eta(x;t)}{\partial t} - \alpha^\eta \, \Delta u^\eta(x;t) = 0, \quad x \in \Omega^\eta, \, t \in \langle 0;\bar{t} \rangle, \quad \eta = A, B, \\
u^\eta(x;0) = u_0^\eta(x), \quad x \in \Omega^\eta, \\
u^\eta(x;t) = g^\eta(x;t), \quad x \in \Gamma_u^\eta, \, t \in \langle 0;\bar{t} \rangle, \\
q^\eta(x;t) = -k^\eta \frac{\partial u^\eta(x;t)}{\partial n^\eta} = h^\eta(x;t), \quad x \in \Gamma_q^\eta, \, t \in \langle 0;\bar{t} \rangle, \\
u^A(x;t) - u^B(x;t) = 0, \quad x \in \Gamma_c, \, t \in \langle 0;\bar{t} \rangle, \\
q^A(x;t) + q^B(x;t) = 0, \quad x \in \Gamma_c, \, t \in \langle 0;\bar{t} \rangle.
\end{gathered} \tag{1}$$

The equations include diffusivity coefficient $\alpha^\eta=k^\eta/(\gamma^\eta\rho^\eta)$ defined by specific heat γ^η, mass density ρ^η and thermal conductivity k^η. The function $q^\eta(x;t)$ determined by the normal derivative of the temperature field introduces heat flux density along the boundary. The split of each boundary Γ^η into three non-overlapping parts due to the boundary and interface conditions can be written as $\Gamma^\eta = \Gamma_u^\eta \cup \Gamma_q^\eta \cup \Gamma_c$. The functions $g^\eta(x;t)$ and $h^\eta(x;t)$ introduce given boundary conditions, while the function $u_0^\eta(x)$ defines the initial condition.

When a problem of heat conduction is to be solved by BIEs, the fundamental solution of the pertinent differential equation eqn. $(1)_1$ is required. This is the solution of eqn. $(1)_1$ at the point x of the equation, where the right hand side contains a point pulse at y and time instance τ, instead of zero. The function and its normal derivatives are given as follows:

$$\begin{gathered}
U^\eta(x,y;t-\tau) = \frac{\alpha^\eta \exp\left(-\frac{|x-y|^2}{4\alpha^\eta(t-\tau)}\right)}{k^\eta\left(4\pi\alpha^\eta(t-\tau)\right)^{\frac{d}{2}}}, \; t \geq \tau, \\
Q^\eta(x,y;t-\tau) = Q^{\eta^*}(y,x;t-\tau) = -k^\eta \frac{\partial U^\eta(x,y;t-\tau)}{\partial n_y^\eta}, \quad D^\eta(x,y;t-\tau) = k^{\eta^2} \frac{\partial^2 U^\eta(x,y;t-\tau)}{\partial n_x^\eta \partial n_y^\eta}.
\end{gathered} \tag{2}$$

They will be used in the next section to introduce the energy functional and the kernels of the resulting BIEs.

3 Variational formulation

The SGBEM approach is usually connected with a variational principle based on a boundary saddle-point quadratic functional, the time dependent problems need it to be convolutive in time, see Bonnet *et al.* [2]. Let us introduce the boundary energy functional Π, established by Carini *et al.* [6] and modified here for a different treatment of the interface conditions, as a function of boundary temperatures and flux densities

$$\begin{aligned}\Pi\left(u^A,u^B,q^A,q^B\right)=&-\sum_{\eta=A,B}\left\{\frac{1}{2}\int\limits_{\Gamma_{uc}^\eta}\int\limits_0^{\bar t} q^\eta\left(x;\bar t-t\right)\int\limits_{\Gamma_{uc}^\eta} U^\eta\left(x,y;t\right)*q^\eta\left(y;t\right)\mathrm{d}S_y\,\mathrm{d}t\mathrm{d}S_x+\right.\\&+\tfrac{1}{2}\int\limits_{\Gamma_{qc}^\eta}\int\limits_0^{\bar t} u^\eta\left(x;\bar t-t\right)\int\limits_{\Gamma_{qc}^\eta} D^\eta\left(x,y;t\right)*u^\eta\left(y;t\right)\mathrm{d}S_y\,\mathrm{d}t\mathrm{d}S_x-\\&\left.-\int\limits_{\Gamma_{uc}^\eta}\int\limits_0^{\bar t} q^\eta\left(x;\bar t-t\right)\int\limits_{\Gamma_{qc}^\eta} Q^\eta\left(x,y;t\right)*u^\eta\left(y;t\right)\mathrm{d}S_y\,\mathrm{d}t\mathrm{d}S_x\right\}-\\&-\frac{1}{2}\int\limits_{\Gamma_c}\int\limits_0^{\bar t}\left[q^A\left(x;\bar t-t\right)\left(u^A\left(x;t\right)-u^B\left(x;t\right)\right)-u^B\left(x;\bar t-t\right)\left(q^A\left(x;t\right)+q^B\left(x;t\right)\right)\right]\mathrm{d}t\mathrm{d}S_x-\\&-\sum_{\eta=A,B}\left\{\int\limits_{\Gamma_{uc}^\eta}\int\limits_0^{\bar t} q^\eta\left(x;\bar t-t\right)\hat g^\eta\left(x;t\right)\mathrm{d}t\mathrm{d}S_x+\int\limits_{\Gamma_{qc}^\eta}\int\limits_0^{\bar t} u^\eta\left(x;\bar t-t\right)\hat h^\eta\left(x;t\right)\mathrm{d}t\mathrm{d}S_x\right\}.\end{aligned}\tag{3}$$

The terms $\hat g^\eta$ and $\hat h^\eta$ are defined by the prescribed boundary values, eqns. $(1)_{2,3,4}$,

$$\begin{aligned}\hat g^\eta\left(x;t\right)=&\int\limits_{\Gamma_q^\eta} U^\eta\left(x,y;t\right)*h^\eta\left(y;t\right)\mathrm{d}S_y-\text{p.v.}\int\limits_{\Gamma_u^\eta} Q^\eta\left(x,y;t\right)*g^\eta\left(y;t\right)\mathrm{d}S_y\\&+\rho\gamma\int\limits_{\Omega^\eta} U^\eta\left(x,y;t\right)u_0^\eta\left(y\right)\mathrm{d}y-c_u^\eta\left(x\right)g^\eta\left(x;t\right),\\\hat h^\eta\left(x;t\right)=&-\text{p.v.}\int\limits_{\Gamma_q^\eta} Q^{\eta*}\left(x,y;t\right)*h^\eta\left(y;t\right)\mathrm{d}S_y+\text{f.p.}\int\limits_{\Gamma_u^\eta} D^\eta\left(x,y;t\right)*g^\eta\left(y;t\right)\mathrm{d}S_y\\&-\rho\gamma\int\limits_{\Omega^\eta} Q^{\eta*}\left(x,y;t\right)u_0^\eta\left(y\right)\mathrm{d}y+c_q^\eta\left(x\right)h^\eta\left(x;t\right).\end{aligned}\tag{4}$$

If $x\in\Gamma_S^\eta$, the free term $c_r^\eta(x)$ is equal to one half along Γ_r^η and vanishes elsewhere on Γ^η for any $r=u,q,c$ or their combination. The marks 'p.v.' and 'f.p.' refer to the Cauchy principle value and the Hadamard finite part, respectively, the methods of strongly and hyper singular integral evaluation.

The weak solution of eqn. (1) can be obtained from the first variation of the energy functional Π, it may provide the BIEs and also the interface conditions. A

slight rearrangement of the terms appearing in the first variation renders the relation

$$
\begin{aligned}
&\delta\Pi\left(u^A,u^B,q^A,q^B;\delta u^A,\delta u^B,\delta q^A,\delta q^B\right)=\\
&-\sum_{\eta=A,B}\left\{\int_{\Gamma_{uc}^{\eta}}\int_0^{\bar t}\delta q^{\eta}\left(x;\bar t-t\right)\left(\int_{\Gamma_{uc}^{\eta}}U^{\eta}\left(x,y;t\right)*q^{\eta}\left(y;t\right)\mathrm{d}S_y-\int_{\Gamma_{qc}^{\eta}}Q^{\eta}\left(x,y;t\right)*u^{\eta}\left(y;t\right)\mathrm{d}S_y\right)\mathrm{d}t\mathrm{d}S_x+\right.\\
&\left.+\int_{\Gamma_{qc}^{\eta}}\int_0^{\bar t}\delta u^{\eta}\left(x;\bar t-t\right)\left(-\int_{\Gamma_{uc}^{\eta}}Q^{\eta *}\left(x,y;t\right)*q^{\eta}\left(y;t\right)\mathrm{d}S_y+\int_{\Gamma_{qc}^{\eta}}D^{\eta}\left(x,y;t\right)*u^{\eta}\left(y;t\right)\mathrm{d}S_y\right)\mathrm{d}t\mathrm{d}S_x\right\}-\\
&-\int_{\Gamma_c}\int_0^{\bar t}\left[\delta q^A\left(x;\bar t-t\right)\left(\tfrac{1}{2}u^A\left(x;t\right)-u^B\left(x;t\right)\right)+\tfrac{1}{2}\delta u^A\left(x;\bar t-t\right)q^A\left(x;t\right)\right]\mathrm{d}t\mathrm{d}S_x+\\
&+\int_{\Gamma_c}\int_0^{\bar t}\left[\delta u^B\left(x;\bar t-t\right)\left(q^A\left(x;t\right)+\tfrac{1}{2}q^B\left(x;t\right)\right)+\tfrac{1}{2}\delta q^B\left(x;\bar t-t\right)u^B\left(x;t\right)\right]\mathrm{d}t\mathrm{d}S_x-\\
&-\sum_{\eta=A,B}\left\{\int_{\Gamma_{uc}^{\eta}}\int_0^{\bar t}\delta q^{\eta}\left(x;\bar t-t\right)\hat g^{\eta}\left(x;t\right)\mathrm{d}t\mathrm{d}S_x+\int_{\Gamma_{qc}^{\eta}}\int_0^{\bar t}\delta u^{\eta}\left(x;\bar t-t\right)\hat h^{\eta}\left(x;t\right)\mathrm{d}t\mathrm{d}S_x\right\}.
\end{aligned}
\tag{5}
$$

The stationary point of the functional Π determined by its vanishing first variation provides the BIEs:

$$
\begin{aligned}
0&=\int_{\Gamma_{uc}^{\eta}}U^{\eta}\left(x,y;t\right)*q^{\eta}\left(y;t\right)\mathrm{d}S_y-\text{p.v.}\int_{\Gamma_{qc}^{\eta}}Q^{\eta}\left(x,y;t\right)*u^{\eta}\left(y;t\right)\mathrm{d}S_y-c_c^{\eta}\left(x\right)u^{\eta}\left(x;t\right)+\hat g^{\eta}\left(x;t\right),\\
0&=-\text{p.v.}\int_{\Gamma_{uc}^{\eta}}Q^{\eta *}\left(x,y;t\right)*q^{\eta}\left(y;t\right)\mathrm{d}S_y+\text{f.p.}\int_{\Gamma_{qc}^{\eta}}D^{\eta}\left(x,y;t\right)*u^{\eta}\left(y;t\right)\mathrm{d}S_y+c_c^{\eta}\left(x\right)q^{\eta}\left(x;t\right)+\hat h^{\eta}\left(x;t\right).
\end{aligned}
\tag{6}
$$

Notice that for points x from to the interface Γ_c the free term contains an unknown function, while the terms $\hat g^{\eta}$ and $\hat h^{\eta}$ defined in eqn. (4) do not contain this free term for interface points. It also makes true a weak representation of interface conditions eqns. $(1)_{5,6}$

$$
\begin{aligned}
0&=\int_{\Gamma_c}\int_0^{\bar t}\delta q^A\left(x;\bar t-t\right)\left(u^A\left(x;t\right)-u^B\left(x;t\right)\right)\mathrm{d}t\mathrm{d}S_x,\\
0&=\int_{\Gamma_c}\int_0^{\bar t}\delta u^B\left(x;\bar t-t\right)\left(q^A\left(x;t\right)+q^B\left(x;t\right)\right)\mathrm{d}t\mathrm{d}S_x.
\end{aligned}
\tag{7}
$$

This weak form of the interface conditions should be seen in view of Vodička *et al.* [8]: the compatibility condition eqn. $(7)_1$ is satisfied with respect to sub-domain Ω^A, $u^B\left(x;t\right)$ being assumed as a known function, on the contrary, the flux equilibrium condition eqn. $(7)_2$ is satisfied with respect to sub-domain Ω^B and with $q^A\left(x;t\right)$ supposed to be given.

4 Numerical solution

The time variable will be treated in a way different from that one used for space variables. Therefore, there appears a difference also in the treatment of the weight functions in eqn. (5). First, let us suppose that the test function includes

an impulse at the time $\tau \in \langle 0;\bar{t}\rangle$, so that it can be rewritten in a weak form with respect only to the space variables

$$
\begin{aligned}
0 = &\int_{\Gamma_u^A} \delta q^A(x)\left(\int_{\Gamma_{uc}^A} U^A(x,y;\tau) * q^A(y;\tau)\,\mathrm{d}S_y - \int_{\Gamma_{qc}^A} Q^A(x,y;\tau) * u^A(y;\tau)\,\mathrm{d}S_y + \hat{g}^A(x;\tau)\right)\mathrm{d}S_x + \\
&+\int_{\Gamma_q^A} \delta u^A(x)\left(-\int_{\Gamma_{uc}^A} Q^{A*}(x,y;\tau) * q^A(y;\tau)\,\mathrm{d}S_y + \int_{\Gamma_{qc}^A} D^A(x,y;\tau) * u^A(y;\tau)\,\mathrm{d}S_y + \hat{h}^A(x;\tau)\right)\mathrm{d}S_x + \\
&+\int_{\Gamma_c} \delta q^A(x)\left(\int_{\Gamma_{uc}^A} U^A(x,y;\tau) * q^A(y;\tau)\,\mathrm{d}S_y - \right. \\
&\qquad \left. - \int_{\Gamma_{qc}^A} Q^A(x,y;\tau) * u^A(y;\tau)\,\mathrm{d}S_y + \tfrac{1}{2}u^A(x;\tau) - u^B(x;\tau) + \hat{g}^A(x;\tau)\right)\mathrm{d}S_x + \\
&+\int_{\Gamma_c} \delta u^A(x)\left(-\int_{\Gamma_{uc}^A} Q^{A*}(x,y;\tau) * q^A(y;\tau)\,\mathrm{d}S_y + \tfrac{1}{2}q^A(x;\tau) + \right. \\
&\qquad \left. + \int_{\Gamma_{qc}^A} D^A(x,y;\tau) * u^A(y;\tau)\,\mathrm{d}S_y + \hat{h}^A(x;\tau)\right)\mathrm{d}S_x + \\
&+\int_{\Gamma_u^B} \delta q^B(x)\left(\int_{\Gamma_{uc}^B} U^B(x,y;\tau) * q^B(y;\tau)\,\mathrm{d}S_y - \int_{\Gamma_{qc}^B} Q^B(x,y;\tau) * u^B(y;\tau)\,\mathrm{d}S_y + \hat{g}^B(x;\tau)\right)\mathrm{d}S_x + \\
&+\int_{\Gamma_q^B} \delta u^B(x)\left(-\int_{\Gamma_{uc}^B} Q^{B*}(x,y;\tau) * q^B(y;\tau)\,\mathrm{d}S_y + \int_{\Gamma_{qc}^B} D^B(x,y;\tau) * u^B(y;\tau)\,\mathrm{d}S_y + \hat{h}^B(x;\tau)\right)\mathrm{d}S_x + \\
&+\int_{\Gamma_c} \delta q^B(x)\left(\int_{\Gamma_{uc}^B} U^B(x,y;\tau) * q^B(y;\tau)\,\mathrm{d}S_y - \right. \\
&\qquad \left. - \int_{\Gamma_{qc}^B} Q^B(x,y;\tau) * u^B(y;\tau)\,\mathrm{d}S_y - \tfrac{1}{2}u^B(x;\tau) + \hat{g}^B(x;\tau)\right)\mathrm{d}S_x + \\
&+\int_{\Gamma_c} \delta u^B(x)\left(-q^A(x;\tau) - \int_{\Gamma_{uc}^B} Q^{B*}(x,y;\tau) * q^B(y;\tau)\,\mathrm{d}S_y - \tfrac{1}{2}q^B(x;\tau) + \right. \\
&\qquad \left. + \int_{\Gamma_{qc}^B} D^B(x,y;\tau) * u^B(y;\tau)\,\mathrm{d}S_y + \hat{h}^B(x;\tau)\right)\mathrm{d}S_x .
\end{aligned}
\tag{8}
$$

The convolution can be evaluated numerically, see Lubich [3], by a quadrature formula whose weights are determined with the help of Laplace transform $\mathcal{L}(f)$ of a function f

$$
\mathcal{L}\left(f(t)\right)(s) = \int_0^{+\infty} f(t)\exp(-st)\,\mathrm{d}t \tag{9}
$$

and a backward difference formula of order $p \leq 6$ for ordinary differential equations with the generating function δ, see below eqn. (11).

Let us rewrite the space double integrals in eqn. (8), using a mask integral kernel Z^{η} instead of the pertinent fundamental kernels U^{η}, Q^{η}, D^{η}. The approximation of the convolution at time $\tau=nt_h$, where $t_h=\overline{t}/N_t$ is a time step and N_t is the total number of time steps, renders

$$\int_{\Gamma_s^{\eta}} \delta v^{\eta}(x) \int_{\Gamma_r^{\eta}} Z^{\eta}(x,y;\tau) * w^{\eta}(y;\tau)\,\mathrm{d}S_y\,\mathrm{d}S_x \cong \int_{\Gamma_s^{\eta}} \int_{\Gamma_r^{\eta}} \delta v^{\eta}(x) \sum_{j=0}^{n} \mathcal{Z}_{n-j}^{\eta}(x,y)\, w_j^{\eta}(y)\mathrm{d}S_y\,\mathrm{d}S_x. \tag{10}$$

The quadrature weight functions $\mathcal{Z}_n^{\eta}$ are the coefficients of the power series expansion associated to the Laplace transform of the pertinent integral kernel Z^{η} evaluated at a point depending on the used backward difference formula

$$\sum_{n=0}^{+\infty} \mathcal{Z}_n^{\eta}(x,y)\,\xi^n = \mathcal{L}\left(Z^{\eta}(x,y;\tau)\right)\left(\frac{\delta(\xi)}{t_h}\right), \quad |\xi|<1, \quad \delta(\xi)=\sum_{m=1}^{p}\frac{(1-\xi)^m}{m}. \tag{11}$$

The details of the quadrature weight function calculation can be found in [3]. The solution (either $u^{\eta}(x;t)$ or $q^{\eta}(x;t)$) at j-th time step is denoted by the mask function $w_j^{\eta}(y)=w^{\eta}(y;\,j\,t_h)$.

The numerical solution of eqn. (8) by the Symmetric Galerkin Boundary Element Method includes division of the boundaries Γ^{η} into boundary elements. The simplest way of discretization suggests conforming isoparametric elements. The approximation of the functions $w_j^{\eta}(x)$ and the choice of weight functions in eqn. (8) can be written in the following form

$$w_j^{\eta}(x) \cong \sum_{k=1}^{N_w^{\eta}} \phi_w^{\eta k}(x)\,\mathrm{w}_{\mathrm{j}}^{\eta k}, \quad \delta v^{\eta}(x)=\phi_v^{\eta l}(x),\ l=1,\ldots,N_v^{\eta}. \tag{12}$$

The functions $\varphi_w^{\eta k}(x)$ are the nodal shape functions, according to the discretization made, for the approximation $\mathrm{w}_j^{\eta k}$ of the nodal values of the function $w_j^{\eta}(x)$, N_w^{η} is the number of nodal unknowns pertinent to function $w_j^{\eta}(x)$. The eqn. (8) can be written, after an appropriate reordering of the terms according to given and unknown data in the n-th temporal step, as follows:

$$\begin{aligned}
&-\left(\mathbf{U}_{uu}^{\eta}\right)_0\left(\mathbf{q}_u^{\eta}\right)_n+\left(\mathbf{Q}_{uq}^{\eta}\right)_0\left(\mathbf{u}_q^{\eta}\right)_n-\left(\mathbf{U}_{uc}^{\eta}\right)_0\left(\mathbf{q}_c^{\eta}\right)_n+\left(\mathbf{Q}_{uc}^{\eta}\right)_0\left(\mathbf{u}_c^{\eta}\right)_n=\\
&\quad=e_n\left(\hat{\mathbf{g}}_u^{\eta}\right)_n-\sum_{j=0}^{n-1}\left[-\left(\mathbf{U}_{uu}^{\eta}\right)_{n-j}\left(\mathbf{q}_u^{\eta}\right)_j+\left(\mathbf{Q}_{uq}^{\eta}\right)_{n-j}\left(\mathbf{u}_q^{\eta}\right)_j-\left(\mathbf{U}_{uc}^{\eta}\right)_{n-j}\left(\mathbf{q}_c^{\eta}\right)_j+\left(\mathbf{Q}_{uc}^{\eta}\right)_{n-j}\left(\mathbf{u}_c^{\eta}\right)_j\right],\\
&\left(\mathbf{Q}_{qu}^{\eta*}\right)_0\left(\mathbf{q}_u^{\eta}\right)_n-\left(\mathbf{D}_{qq}^{\eta}\right)_0\left(\mathbf{u}_q^{\eta}\right)_n+\left(\mathbf{Q}_{qc}^{\eta*}\right)_0\left(\mathbf{q}_c^{\eta}\right)_n-\left(\mathbf{D}_{qc}^{\eta}\right)_0\left(\mathbf{u}_c^{\eta}\right)_n=\\
&\quad=e_n\left(\hat{\mathbf{h}}_q^{\eta}\right)_n-\sum_{j=0}^{n-1}\left[\left(\mathbf{Q}_{qu}^{\eta*}\right)_{n-j}\left(\mathbf{q}_u^{\eta}\right)_j-\left(\mathbf{D}_{qq}^{\eta}\right)_{n-j}\left(\mathbf{u}_q^{\eta}\right)_j+\left(\mathbf{Q}_{qc}^{\eta*}\right)_{n-j}\left(\mathbf{q}_c^{\eta}\right)_j-\left(\mathbf{D}_{qc}^{\eta}\right)_{n-j}\left(\mathbf{u}_c^{\eta}\right)_j\right],
\end{aligned}$$

$$
\begin{aligned}
&-\left(\mathbf{U}_{cu}^{A}\right)_0\left(\mathbf{q}_u^{A}\right)_n+\left(\mathbf{Q}_{cq}^{A}\right)_0\left(\mathbf{u}_q^{A}\right)_n-\left(\mathbf{U}_{cc}^{A}\right)_0\left(\mathbf{q}_c^{A}\right)_n+\left[\left(\mathbf{Q}_{cc}^{A}\right)_0-\tfrac{1}{2}\mathbf{M}_c^{AA}\right]\left(\mathbf{u}_c^{A}\right)_n+\mathbf{M}_c^{AB}\left(\mathbf{u}_c^{B}\right)_n=\\
&\qquad=e_n\left(\hat{\mathbf{g}}_c^{A}\right)_n-\sum_{j=0}^{n-1}\left[-\left(\mathbf{U}_{cu}^{A}\right)_{n-j}\left(\mathbf{q}_u^{A}\right)_j+\left(\mathbf{Q}_{cq}^{A}\right)_{n-j}\left(\mathbf{u}_q^{A}\right)_j-\left(\mathbf{U}_{cc}^{A}\right)_{n-j}\left(\mathbf{q}_c^{A}\right)_j+\left(\mathbf{Q}_{cc}^{A}\right)_{n-j}\left(\mathbf{u}_c^{A}\right)_j\right],\\
&\left(\mathbf{Q}_{cu}^{A*}\right)_0\left(\mathbf{q}_u^{A}\right)_n-\left(\mathbf{D}_{cq}^{A}\right)_0\left(\mathbf{u}_q^{A}\right)_n+\left[\left(\mathbf{Q}_{cc}^{A*}\right)_0-\tfrac{1}{2}\mathbf{M}_c^{AA}\right]\left(\mathbf{q}_c^{A}\right)_n-\left(\mathbf{D}_{cc}^{A}\right)_0\left(\mathbf{u}_c^{A}\right)_n=\\
&\qquad=e_n\left(\hat{\mathbf{h}}_c^{A}\right)_n-\sum_{j=0}^{n-1}\left[\left(\mathbf{Q}_{cu}^{A*}\right)_{n-j}\left(\mathbf{q}_u^{A}\right)_j-\left(\mathbf{D}_{cq}^{A}\right)_{n-j}\left(\mathbf{u}_q^{A}\right)_j+\left(\mathbf{Q}_{cc}^{A*}\right)_{n-j}\left(\mathbf{q}_c^{A}\right)_j-\left(\mathbf{D}_{cc}^{A}\right)_{n-j}\left(\mathbf{u}_c^{A}\right)_j\right],\\
&-\left(\mathbf{U}_{cu}^{B}\right)_0\left(\mathbf{q}_u^{B}\right)_n+\left(\mathbf{Q}_{cq}^{B}\right)_0\left(\mathbf{u}_q^{B}\right)_n-\left(\mathbf{U}_{cc}^{B}\right)_0\left(\mathbf{q}_c^{B}\right)_n+\left[\left(\mathbf{Q}_{cc}^{B}\right)_0+\tfrac{1}{2}\mathbf{M}_c^{BB}\right]\left(\mathbf{u}_c^{B}\right)_n=\\
&\qquad=e_n\left(\hat{\mathbf{g}}_c^{B}\right)_n-\sum_{j=0}^{n-1}\left[-\left(\mathbf{U}_{cu}^{B}\right)_{n-j}\left(\mathbf{q}_u^{B}\right)_j+\left(\mathbf{Q}_{cq}^{B}\right)_{n-j}\left(\mathbf{u}_q^{B}\right)_j-\left(\mathbf{U}_{cc}^{B}\right)_{n-j}\left(\mathbf{q}_c^{B}\right)_j+\left(\mathbf{Q}_{cc}^{B}\right)_{n-j}\left(\mathbf{u}_c^{B}\right)_j\right],\\
&\left(\mathbf{Q}_{cu}^{B*}\right)_0\left(\mathbf{q}_u^{B}\right)_n-\left(\mathbf{D}_{cq}^{B}\right)_0\left(\mathbf{u}_q^{B}\right)_n+\left[\left(\mathbf{Q}_{cc}^{B*}\right)_0+\tfrac{1}{2}\mathbf{M}_c^{BB}\right]\left(\mathbf{q}_c^{B}\right)_n-\left(\mathbf{D}_{cc}^{B}\right)_0\left(\mathbf{u}_c^{B}\right)_n+\mathbf{M}_c^{BA}\left(\mathbf{q}_c^{A}\right)_n=\\
&\qquad=e_n\left(\hat{\mathbf{h}}_c^{B}\right)_n-\sum_{j=0}^{n}\left[\left(\mathbf{Q}_{cu}^{B*}\right)_{n-j}\left(\mathbf{q}_u^{B}\right)_j-\left(\mathbf{D}_{cq}^{B}\right)_{n-j}\left(\mathbf{u}_q^{B}\right)_j+\left(\mathbf{Q}_{cc}^{B*}\right)_{n-j}\left(\mathbf{q}_c^{B}\right)_j-\left(\mathbf{D}_{cc}^{B}\right)_{n-j}\left(\mathbf{u}_c^{B}\right)_j\right].
\end{aligned}
\tag{13}
$$

The symbols $\left(\mathbf{Z}_{sr}^{\eta}\right)_i, \mathbf{M}_{sr}^{\eta\sigma}$ denote matrices, whose elements are defined respectively by the relations

$$
\left(Z_{sr}^{\eta}\right)_i^{lk}=\int_{\Gamma_s^{\eta}}\int_{\Gamma_r^{\eta}}\phi_v^{\eta\,l}(x)\mathcal{Z}_i^{\eta}(x,y)\phi_w^{\eta\,k}(y)\,\mathrm{d}S_y\,\mathrm{d}S_x,\quad \left(\mathrm{M}_s^{\eta\sigma}\right)^{lk}=\int_{\Gamma_s^{\eta}}\phi_v^{\eta\,l}(x)\phi_w^{\sigma\,k}(x)\,\mathrm{d}S_x.
\tag{14}
$$

The nodal values either prescribed or not are gathered into vectors $\left(\mathbf{w}_r^{\eta}\right)_j$, with subscripts $s,r=u,t,c$ introduced according to boundaries' splits.

It should be clearly seen that the solution at each time step uses the same left hand side matrix with index 0 which is symmetric. Therefore, matrix factorization has to be performed only once. However, at each time step, the right hand side has to be evaluated from the results of the previous steps. The vectors $\left(\hat{\mathbf{g}}_r^{\eta}\right)_j$ and $\left(\hat{\mathbf{h}}_r^{\eta}\right)_j$ contain nodal data given by the boundary conditions and appropriately evaluated by eqn. (4). The numbers e_n are the end-point correction weights of the p-th order Newton-Gregory quadrature formula introduced in order to obtain the convergence property according to [3]. Otherwise they can be set to unity.

5 Examples

Although the developed formulation is valid in 3D space as well, for the sake of simplicity we confine ourselves only to the 2D examples. Nevertheless, the algorithm presented here only for a split of the solution domain into two parts can be applied also for domains containing more sub-domains. An example therefore contains three sub-domains to demonstrate this possibility.

First, let us consider a square divided into two parts as shown on the left picture in Figure 1. This example has been taken to demonstrate the properties of the solution transfer across the interface. The material parameters have been set to unity and all calculations have been done without units. The initial and boundary conditions have been set according to the relations

$$u\left(\left(x_1,x_2\right);0\right)=0,\quad u\left(\left(x_1,0\right);t\right)=0,\quad q\left(\left(0,x_2\right);t\right)=0,$$
$$q\left(\left(2,x_2\right);t\right)=-4x_2^2\left(1-\exp\left(-t\right)\right),\quad q\left(\left(x_1,2\right);t\right)=-4x_1^2\left(1-\exp\left(-t\right)\right). \tag{15}$$

The problem is solved up to the unit total time $\bar{t}$.

The analytical solution is known, at least in the form of a series-expansion so that a comparison of analytical and numerical solutions has been enabled. The interface has been defined by a cubic spline passing through the points E, S_i and F, with: S_1[0.5;0.4], S_2[1.0;1.1], S_3[1.5;1.6]. Numerical solutions have been compared for three boundary element meshes. The coarsest mesh consists of four linear elements along the long segments of the outer contour of each sub-domain and one along the short ones. Five elements have been put along both sides of the interface meshed conformingly and a five-to-six non-conforming interface mesh has been chosen in the other case. The mesh has been then two times refined doubling at each step the number of elements. With respect to the time variable, the total time $\bar{t}$ has been split into four equal time-steps for the first boundary element mesh. The time step has been also halved for the subsequent meshes. The order p of the backward difference formula, see also eqn. (11), has been two.

In this example, the behavior of the errors with respect to the refinement can be studied as long as the analytical solution can be calculated, too. The graphs of Figure 2 and Figure 3 show the distribution of errors relatively to the magnitude of the overall analytical solution obtained for conforming and non-conforming interface meshes, respectively, of temperatures u and heat fluxes q plotted against the arc length l of the interface measured from the point E. The letters in the legends refer to the letters which distinguish the sub-domains on Figure 1 (left) and the numbers denote the smallest number of the elements used in the interface meshes. The superscripts 'num' and 'ex' refer to numerical and analytical results, respectively.

The results of conforming meshes are naturally smoother than those of non-conforming meshes, their magnitudes, however, do not differ significantly.

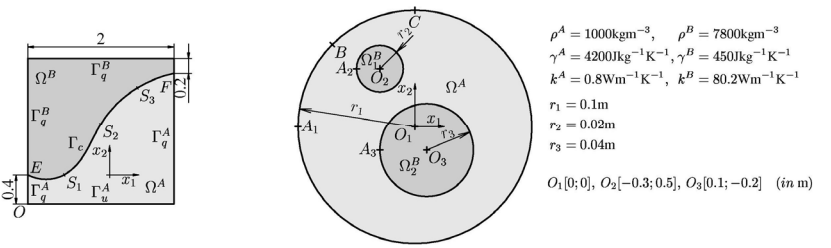

Figure 1: Geometry of the examples.

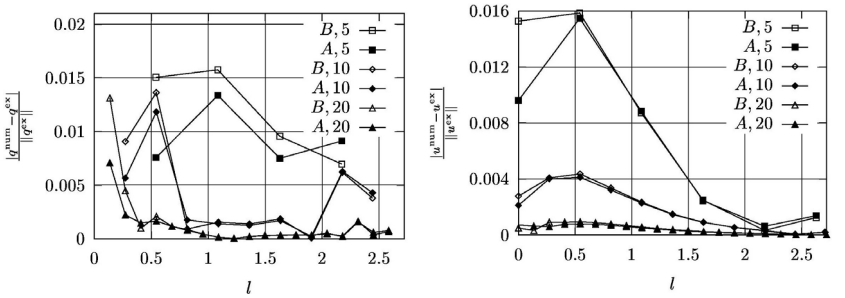

Figure 2: Errors for $t = \bar{t}$, conforming meshes.

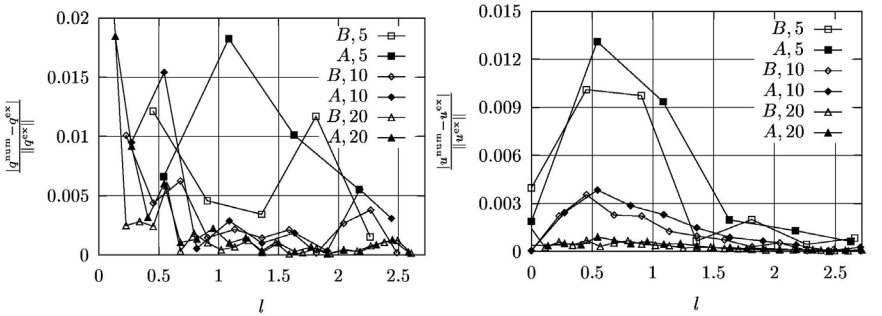

Figure 3: Errors for $t = \bar{t}$, non-conforming meshes.

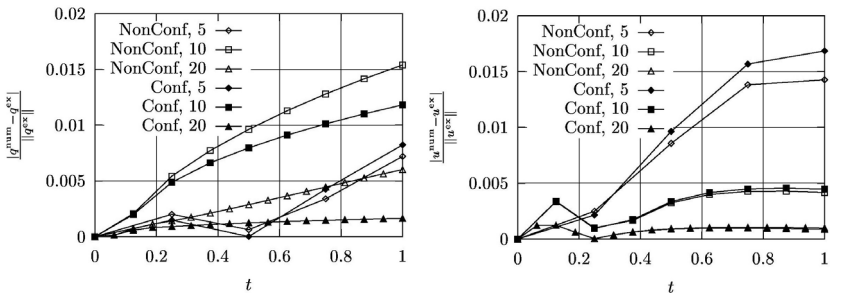

Figure 4: Errors at the point S_3.

Moreover, it can be seen that the errors diminish approximately four times for each refinement, especially for temperatures, which confirms the expected quadratic convergence of the errors, see Lubich and Schneider [3]. The equilibrium and compatibility of the data, supposed to be satisfied in a weak form, eqn. (5), are satisfied, with an excellent agreement for conforming meshes and a quite good fit also for the non-conforming meshes.

The evolution of the errors in time at the point S_3 is shown on Figure 4, where both conforming and non-conforming mesh results are presented. The convergence observations from the previous paragraph can be repeated. The quadratic convergence can be observed, here caused by the choice p=2, see

Lubich and Schneider [3], a bit lower order appeared for the heat fluxes, especially non-conforming mesh. Notice that the coarsest mesh behaves differently in heat fluxes, probably due to the fact that it is actually rather coarse, with respect to the curvature of the interface and its approximation by linear isoparametric space elements.

In the second example, let us consider more realistic material parameters and real units, see Figure 1 (right). The initial and boundary conditions have been set as follows: the initial conditions have been given by different constant temperatures in each of the sub-domains: u_0^A=290K, u_0^{B1}=280K, u_0^{B2}=320K with vanishing flux prescribed along the outer contour. The problem is solved up to the total time $\bar{t}$=1h.

The boundary element mesh contains equally distributed 32 linear elements along each circle of the boundary or the interface, with an exception of the upper half circles of the interfaces with respect to B sub-domains, which contain 20 elements. The time step has been taken such that 16 steps have been done to reach $\bar{t}$ with the order p=2 in the algorithm of the convolution quadrature.

The results shown on Figure 5 demonstrate the evolution of both calculated functions along the interfaces evaluated with respect to the inclusions at the time instances $t=\alpha\bar{t}$. The data are plotted starting respectively from points A_2, A_3 counter-clockwise, the arc angle is denoted by φ. No difference in the solution appeared between the upper and lower half circles, possibly caused by the different meshing properties supposed.

The graphs confirm expected behavior of the solution, where the heat flux shows the concentration at inclusion points which are closest to each other. The

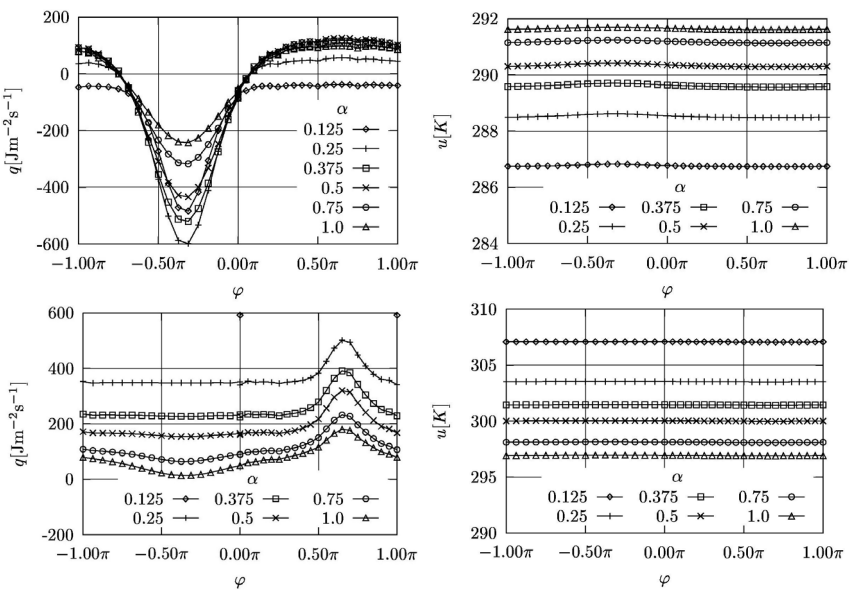

Figure 5: Solutions along the interfaces: $\Omega^A \leftrightarrow \Omega^B{}_1$ (top), $\Omega^A \leftrightarrow \Omega^B{}_2$ (bottom).

evolution of temperature is also natural, as depending on the size of the inclusion and its position they tend towards the expected values of a stationary solution.

6 Conclusions

A solution of interface heat conduction IBVP by a Galerkin boundary element technique has been discussed. In the proposed method, the two crucial points of the solution, treatment of the interface relations and time dependence, have been resolved satisfactorily by applying a variational principle to obtain a weak form of the interface conditions for the former crucial point and by utilizing a convolution quadrature method for obtaining a time-domain solution as the latter one. It was demonstrated by two simple but problem describing examples. The results provoke the further demonstration of the method in a wider range of problems with interfaces in a forthcoming paper.

Acknowledgement

The work has been supported by the grants VEGA No 1/4198/07 and 1/4160/07.

References

[1] Costabel, M., Time-dependent problems with boundary integral equation method (Chapter 25). *Encyclopedia of Computational Mechanics*, John Wiley & Sons, Eds. Stein, de Borst, Hughes. vol. 1, 2004.
[2] Bonnet, M., Maier, G., Polizzotto, C., Symmetric Galerkin boundary element method. *Applied Mechanics Review,* **5**, pp.669–704, 1998.
[3] Lubich, C., Schneider R., Time discretization of parabolic boundary integral equations. *Numerishe Mathematik,* **63**, pp. 455—481, 1992.
[4] Hsiao, G.C., Steinbach, O., Wendland, W.L., Domain decomposition methods via boundary integral equations. *Journal of Computations and Applied Mathematics,* **125**, pp.521–537, 2000.
[5] Wohlmuth, B.I., Discretization Methods and Iterative Solvers Based on Domain Decomposition. *Lecture Notes in Computational Science and Engineering,* vol.17, Springer: Berlin, 2001.
[6] Carini, A., Diligenti, M., Maier, G., Symmetric boundary integral formulations of transient heat conduction: saddle-point theorems for BE analysis and BE-FE coupling. *Archives of Mechanics*, **49**, pp. 253–283, 1997.
[7] Langer, U., Steinbach, O., Boundary element tearing and interconnecting method. *Computing*, **71**, pp. 205–228, 2003.
[8] Vodička, R., Mantič, V., París, F., Symmetric variational formulation of BIE for domain decomposition problems in elasticity - an SGBEM approach for nonconforming discretizations of curved interfaces. *CMES – Computer Modeling in Engineering and Science,* **17**, pp. 173–203, 2007.
[9] Boer, A. de, Zuijlen, A.H. van, Bijl, H., Review of coupling methods for non-matching meshes. *Computational Methods in Applied Mechanics and Engineering, **196***, pp.1515–1525, 2007.